An Index of Red Tide Mortality on red grouper in the Eastern Gulf of Mexico

David Chagaris and Dylan Sinnickson

SEDAR61-WP-06

17 August 2018

Please cite this document as:

Chagaris, David and Dylan Sinnickson. 2018. An Index of Red Tide Mortality on red grouper in the Eastern Gulf of Mexico. SEDAR61-WP-06. SEDAR, North Charleston, SC. 16 pp.

An Index of Red Tide Mortality on red grouper in the Eastern Gulf of Mexico

David Chagaris and Dylan Sinnickson

University of Florida, IFAS Nature Coast Biological Station and SFRC Fisheries and Aquatic Sciences Program, Gainesville FL.

Introduction

Karenia brevis is a dinoflagellate that causes toxic red tide blooms in the Gulf of Mexico and Southeast U.S. (Steindinger 2009). In the Gulf of Mexico, red tides occur off the coast of Texas and Florida. They are believed to be caused by a sequence of physical and ecological processes that includes phytoplankton succession stage, nutrient and light availability, and upwelling transport (Walsh et al. 2006). When *K. brevis* cells lyse they release brevitoxins that are ingested by fish or absorbed across the gill membranes impacting the nervous and respiratory systems and causing mortality (Landsberg 2002). Severe blooms can result in large fish kills (Flaherty and Landsberg 2011; Smith 1975, 1979; Steidinger and Ingle 1972). Decomposition of dead carcasses turns the water hypoxic and releases nutrients that stimulate bloom growth (Walsh et al. 2009), extending its duration and exasperating the impacts. On the West Florida Shelf (WFS) red tide blooms usually occur along the coast between August and November. They tend to be more frequent earlier in the season for the northern Big Bend region and later for areas south of Tampa Bay. In some years red tides can be extremely severe leading to massive fish kills (Flaherty and Landsberg 2011; Smith 1975, 1979; Steidinger and Ingle 1972), respiratory stress on humans (Kirkpatrick et al. 2004), fishery closures, and impacts to the local economy (Larkin and Adams 2007).

In 2005, a severe bloom formed offshore during September and persisted until December covering a large portion of the WFS and extending into bays and estuaries (Hu et al. 2005; Flaherty and Landsberg 2011). Masses of dead floating groupers (family Serranidae.) were observed offshore in 2005 during the National Marine Fisheries Service (NMFS) bottom longline survey (Walter et al. 2013). In Tampa Bay, the 2005 bloom also resulted in declines in recruitment of popular nearshore species (e.g. spotted seatrout, red drum) and shifts in the fish community structure (Flaherty and Landsberg 2011). Another severe bloom occurred in 1971 causing a severe die-off of fauna on patch reefs located on the inner shelf near Sarasota (Smith 1975, 1979). The mortality rate associated with red tides can be substantial on certain fish species. For gag grouper, red tide mortality (M_{RT}) in 2005 was estimated to be 0.35 and 0.71, in the 2009 and 2014 assessments respectively (SEDAR 2009, 2014), which is 2 to 5 times higher than baseline natural mortality rates. Thus, both models estimated severe, although highly variable, effects of red tide on gag populations. Similarly, red tide was included in the last stock assessment of red grouper and was estimated to kill approximately 43.8% of the total biomass in 2005 (SEDAR 2015).

Following the 2014 gag assessment, the GMFMC SSC recommended an allowable biological catch (ABC) assuming a high M_{RT} in 2014 for a bloom that was occurring in the Big Bend region of Florida (Hu et al. 2015). This recommendation was rejected by the Council. After further evaluation of the spatio-temporal distribution of the red tide, the SSC adjusted the ABC upward by over 3 million pounds for 2015 (GMFMC 2015). Discrepancies in the estimates of M_{RT} by the 2009 and 2014 stock assessments, and the lack of information available to the SSC

when setting future catch limits, highlight the need for independent and timely assessments of red tide effects, or other episodic mortality events, on fisheries resources.

In this study we update the analysis conducted for gag grouper in 2015 (GMFMC 2015) and apply it to red grouper in support of the ongoing SEDAR 61 stock assessment. Our objective is to integrate information describing the spatial extent, duration, and severity of blooms with species distribution maps to generate an index of red tide mortality. Additionally, our intent was to develop a process that can be readily updated in order to provide timely information for management action in years when stock assessments are not conducted.

Methods

To estimate the impacts of red tides on fish populations it is important to consider the size and location of the bloom, along with its severity, duration, and spatial overlap with the species of interest. We developed a spatially explicit approach that uses synoptic satellite imagery to define the spatial extent of blooms, in situ *K. brevis* cell concentrations (cells/liter) to approximate the severity, a spatially explicit ecosystem model to provide the spatial distribution patterns of red grouper, and a logistic mortality response function to impose mortality in each map cell. Each of these components is described in detail in the following sections.

Remote Sensing of Red Tide Blooms

Normalized fluorescence line height (FLH) imagery has been used as a tool to study and monitor algal blooms in southwest Florida coastal waters (Hu et al. 2005; Hu et al. 2015; Soto 2013). FLH is an indicator of algal blooms, both harmful and not, and can also be influenced by sediment resuspension which can cause FLH to be overestimated. Therefore, we used the FLH imagery only to identify the location of potential harmful algal blooms and validated the imagery using *in situ K. brevis* cell concentrations (described below). Maps of monthly and 8-day normalized FLH (mW cm^{-2} μm^{-1} sr^{-1}) measured by the MODIS Aqua satellite (using the 678 nm MODIS instrument band) are available from July 2002 on the NASA Giovanni Interactive Visualization and Analysis website (https://giovanni.gsfc.nasa.gov/giovanni/; Acker and Leptoukh 2007). Monthly maps of FLH from July 2002 to March 2018 were downloaded for the area covering the West Florida Shelf (WFS), from -88° to -81° longitude and 23° to 30.5° latitude at a spatial resolution of 4 km^2. Hu et al. (2005) determined that FLH > 0.012 mW cm^{-2} μm^{-1} sr^{-1} is the threshold for detecting harmful algal blooms. However recent calibrations to the algorithms used to process FLH satellite data resulted in an increase of the detection threshold to 0.02 (Soto 2013; Hu personal communication). Using this threshold, we generated polygons of algal blooms along the WFS each month from July 2002 to March 2018 (Figure 1).

In Situ Karenia brevis Cell Concentrations

The Florida Fish and Wildlife Conservation Commission Fish and Wildlife Research Institute's (FWRI) harmful algal bloom (HAB) group monitors more than 100 locations around the state weekly, twice-monthly or monthly to detect nuisance, harmful and toxic algal blooms, including Florida red tide. Additional information on the FWRI-HAB program can be found at http://myfwc.com/research/redtide/. In brief, FWRI-HAB staff coordinates sample collection with state agencies, local governments and private citizens participating in a volunteer offshore monitoring program. In addition to routine monitoring, HAB staff respond to possible blooms throughout Florida. Following reports of discolored water, respiratory irritation, fish kills, or

dead or stranded marine mammals, HAB staff lead sampling trips or coordinate sampling with the same collaborators they rely on for routine monitoring. This event-response effort varies from year to year, depending on the frequency and duration of blooms. Water samples collected from shore, bridges, piers or boats are returned to the FWRI laboratory in St. Petersburg where researchers examine them under a microscope for HAB species. All data are entered into the HAB historical database.

K. brevis cell concentration (cells/L) data collected by FWRI-HAB were interpolated over the entire WFS using ordinary kriging. For each month and sample location we obtained the maximum observed *K. brevis* cell concentration (Figure 2) and performed ordinary kriging for months when there were at least 5 sites with maximum concentrations greater than or equal to 1,000 cells/L. The 'autoKrige' function from the R package 'automap' was used to fit the variogram model to the log-transformed monthly observed maximum cell concentrations at each sample location. The autoKrige function conveniently tested several variogram model types, including the commonly used spherical, exponential, and matern (M. Stein's parameterization) models, and selected the model with smallest residual sum of squares in the sample variogram (Figure 3). The selected model and data were used to predict cell concentrations over a spatial grid matching the FLH imagery and then back-transformed. Lastly, the kriged maps were clipped to the HAB polygons identified by the FLH detection threshold of 0.02 and resampled to match the resolution of the species distribution maps (Figure 4).

Species Distribution Maps

An Ecopath with Ecosim and Ecospace model (EwE) was previously developed for the WFS to simulate the trophic impacts of harvest policies, identify tradeoffs between reef fish conservation and fishery profits, and evaluate the performance of marine protected areas (Chagaris et al. 2015; Chagaris 2013). The spatial distributions of red grouper biomass on the WFS were predicted by the spatially component Ecospace for 0-1 year olds, 1-3 year olds, and 4+ year olds. The Ecospace habitat capacity model uses habitat layers to alter the amount of available foraging area in each map cell in order to predict spatial distribution patterns (Christensen et al 2014). The WFS Ecospace model extends from 25-30.5° N and 88.5-81° W and consists of 34 rows and 40 columns with a spatial resolution of 10 minutes. Water cells deeper than 250 m are excluded from calculations in the WFS Ecospace model. In the WFS Ecospace model, red grouper were distributed spatially based on relationships to depth and rugosity (as a proxy for bottom structure), and also food availability, and proximity to earlier life stages (Figure 5). The maps of red tide polygons with kriged cell concentrations were then resampled to match the exact spatial extent and resolution of the Ecospace species distribution maps (Figure 4).

Mortality Estimation

A logistic function was used to determine the proportion of biomass that was killed in each grid cell during each month from July 2002 to March 2018, which was the extent of available data at the time this analysis was conducted. The shape of the response function was estimated in order to produce the "known" mortality (i.e. proportion of biomass killed) caused by the 2005 red tide bloom as estimated by the stock assessment which was based on observed declines in abundance indices. The 2015 SEDAR 42 stock assessment estimated the total biomass in 2005 to be 45,012 mt and 19,731 mt was killed by red tides, leading to a red tide mortality (M_{RT}) of 0.438 for 2005. For each month, the response function was applied to

determine the proportion of biomass killed (P_{dead}) in each map cell. The P_{dead} was then multiplied by the biomass of each age stanza in that cell. The killed biomass was subtracted and the surviving biomass in each map cell was passed to the next month's calculation. This essentially allowed for the biomass to be mined down in map cells where red tides persisted for several months. The M_{RT} for each year was then calculated as the proportion of biomass killed, total and by age stanza, over the entire year divided by the biomass at the start of the year. At the beginning of each year, the biomass-at-age was updated with the values corresponding to those from the stock assessment and species distribution maps remained static.

Because there was only one data point for which to fit the response function (the M_{RT} in 2005 from stock assessment), only one parameter could be estimated at a time. Therefore, we converted the two parameter logistic function with inflection point (C_{50}, the cell concentration with a 50% probability of dying) and slope to a one parameter function by scaling the slope to the inflection point based on a fixed value a.

$$P_{dead} = \frac{1}{1 + \left(\frac{x}{C_{50}}\right)^{-\left(\frac{C_{50}}{a}\right)}}$$

We estimated eight different response curves over a values of 1000, 10000, 25000, 50000, 75000, 100000, 200000, and 300000. In these logistic curves, smaller values of a resulted in steeper slopes around the inflection point and larger a resulted in flatter slopes. The eight response functions were then used to predict the mortality due to red tides in all other years.

Results

Summary of Red Tide Events on the WFS

Based on the FLH imagery, the extent and intensity of *K. brevis* blooms varied each year, but generally demonstrated similar seasonal trends. Blooms normally reached their greatest intensity in late summer and early fall and persisted to some extent into January and February. In certain years such as 2005, the extent of blooms was greatest in September and weakened throughout the fall, while in other years, such as 2010, blooms expanded throughout the fall and into the winter of the following year (Figure 7). By March, blooms generally reached their smallest size and remained relatively unchanged until mid-summer.

The 2005 event was by far the largest observed in our data and it broadly impacted most of the WFS throughout a large part of the year (Figure 1). Smaller blooms occurred in 2006, 2012, 2014, and 2016. From 2007 to 2011 there were no severe red tides on the WFS. The 2006 bloom, while spatially restricted, was particularly severe in October and November with estimated *K. brevis* cell concentrations greater than 1 million cells where blooms (>= 10,000 cells/L) were present. Other severe but highly local blooms occurred in late 2012 and early 2013, as well as 2014. Some of these localized blooms included the aforementioned 2014 bloom that was present in the Big Bend region, the 2016 bloom that occurred in the central portion of Florida, and the 2011 bloom that was present in the southern portion of the state.

The FWRI-HAB cell concentration data confirmed that red tide blooms were generally more localized that what the FLH imagery alone would indicate. While the FLH imagery often showed blooms extending along most of the coastline, the *in situ* data confirmed high *K. brevis* counts in much smaller areas within those regions. While background levels of K. brevis

(10,000 cells/L) are present almost year round throughout the time series, there were far fewer months where blooms consisting of >50,000 cells/L were present.

Trends in Red Tide Mortality

The inflection points from the logistic mortality response curves that generated a M_{RT} of 0.438 in 2005 were estimated to range between approximately 140,000 to 220,000 cells/L (Figure 8). The steepest curve exhibited knife-edged mortality response with zero and 100% mortality when *K. brevis* cell concentrations were, respectively, less than or greater to 152,180 cells/L. The flattest curve ($c50$ = 216,111; a = 300,000) resulted in low levels of mortality at even background *K. brevis* concentrations but only moderate mortality at very high cell concentrations. Curves with a parameters less than 1,000 or greater than 300,000 were tested but did not return the 2005 M_{RT} of 0.438.

The analyses demonstrated that 2005 had substantially higher mortality rates than any other year in our study. For all shapes evaluated, 43.8% of the total red grouper biomass was estimated to be killed by red tides in 2005, which is equal to that predicted by the stock assessment (Table 1; Figure 9). The year with the next highest mortality on total biomass was 2006 when a highly toxic but spatially limited bloom was estimated to kill between 7.5% and 10.5% of total red grouper biomass. Beyond those years, the next highest mortality was estimated for 2014, followed by 2011 or 2016 depending on the shape of the curve with mortality ranging between 0.3% and 3.5% of the total biomass killed.

Although the proportion of total biomass killed by red tides was estimated to be low in most years, the estimated mortality was disproportionately higher for younger age stanzas (Figure 9). For age-0 fish, M_{RT} was highest in 2005 (40.9-45.4% of age-0 biomass killed) followed by 2006 (23.0-28.5%). From 2011-2013 M_{RT} on age-0 ranged between 11.5-20% and in 2016 was estimated to be between 6.8-24.3% (Table 2). For older juveniles (ages 1-3), M_{RT} was again highest in 2005 (~50% biomass killed), followed by 2006 (15.8-20.6%). Similar to the pattern observed for age-0 fish, MRT was higher for this age stanza than what that based on total biomass from 2011 to 2013 (4.9-9.6%). In 2016, the loss of age 1-3 year olds was estimated to be between 4.2% and 13.4%.

Discussion

We conclude that for red grouper the percent of total biomass killed by red tides has likely been low in all years since 2002, with the exception of 2005. This is because in most years, the severe blooms are localized and do not overlap substantially with the spatial distribution of the entire red grouper stock biomass. Red tide blooms tend to be present closer to shore while the bulk of red grouper biomass exists offshore. However, disproportionally higher effects were estimated for the younger age classes that occupy nearshore habitats where red bloom generally occur more regularly and with higher severity. The elevated pattern of high mortality on younger ages beginning in 2011 is concerning because it could potentially be impacting current recruitment levels.

It is generally reported by the FWC that concentrations of *K. brevis* between 10,000-100,000 cells/L will results in possible fish kills, and concentrations above 100,000 cells/L will increase the probability of fish kills (http://myfwc.com/redtidestatus). The mortality response curves estimated in this analysis suggest that 50% of biomass in a given location will be killed at

concentrations between 140,000 and 220,000 cells/L. These estimated response functions are well within reason given what is known from past red tide events and observed fish kills.

There are some key caveats and uncertainties associated with this analysis that require additional research. First, we defined the spatial extent of blooms using only sea surface imagery of FLH. If subsurface blooms are present and extend far beyond those observed by satellites, then our estimates of mortality would be biased downwards. Second, bloom toxicity is not well correlated with cell concentrations, such that high *K. brevis* concentrations do not always lead to fish kills and low concentrations may result in large fish kills. Blooms become toxic when the cells undergo lysis, and this happens at a certain stage of bloom maturity which is based on the ambient concentrations of nutrients and competing autotrophs. While we believe that cell concentrations are a reasonable proxy for toxicity, efforts to integrate biology of HABs into the analysis would be a worthwhile endeavor. Third, the spatial distribution maps generated by the Ecospace model have not been formally validated against empirical data, but only qualitatively compared against observations from fisheries independent surveys. The species distribution maps could be improved by using more statistically sound approaches that utilize survey data to validate predicted spatial patterns.

Another way to improve upon this analysis is to further refine the temporal resolution of the analysis. Red tide blooms are highly dynamic and it is possible that the synoptic monthly maps used to define the spatial extent are not always representative of conditions that might lead to fish kills. For example, a severe bloom existing for only a few days may not factor strongly into the monthly average FLH imagery. In fact, there were a few cases where the FWRI-HAB data indicated *K. brevis* cell concentrations > 10,000 was present in areas beyond where FLH values were above the threshold of 0.02, which could be indicative of fine-scale bloom dynamics and/or presence of subsurface blooms. In the future, 8-day or bi-weekly maps might be explored to better represent the spatio-temporal dynamics of red tide blooms. However, there are limitations to consider such as availability of consistent satellite imagery due to cloud cover and the frequency and spatial distribution of *in situ* HAB sampling.

In the future, the analysis should be integrated into a population dynamic or ecosystem modeling approach and fit to spatially explicit abundance estimates. Single-species delay difference models provide a computationally efficient way to simulate numbers and biomass dynamics over spatial grids, and those might prove to be useful for such an application. Efforts are ongoing to integrate red tide maps into an existing Ecospace model of the WFS, utilizing the EwE spatial-temporal framework (EwE-STF) to update environmental driver maps. However EwE-STF currently only allows the environmental drivers to manipulate the foraging capacity in a map cell, which causes fish to either move to more suitable habitat or starve and die. Thus, more work is needed to allow drivers such as red tides (or oil spills) to directly influence mortality across a spatial grid. Ultimately, this will enable us to simulate red tide impacts on fish populations and food webs, while representing movement rates that may allow some species to avoid smaller blooms.

Despite the caveats and limitations described above, we believe the estimated relative trend in red tide mortality is reasonable. We base this conclusion on our assumptions that the FLH imagery does not drastically over- or under-estimate bloom detection, that cell concentrations are a reasonable proxy for bloom toxicity, and that the spatial distribution of red grouper biomass predicted by Ecospace is not far from reality. Finally, an advantage of the approach described here is that it has potential to make near real-time predictions about the effects of ongoing red tide events on fish populations. This is because the satellite imagery and

FWRI-HAB data can be made available within days or weeks and the analysis workflow can be automated to accept new data as they become available and update the time series. This will allow fisheries managers to make timely adjustments without requiring an update to the stock assessment, and will also allow stock assessment scientists a reliable and reproducible index of red tide mortality that may improve model estimation.

Tables

Table 1. Estimated red tide mortality on red grouper from July 2002 to March 2018. Mortality is expressed as the proportion of total biomass killed by red tides for each of the mortality response curves evaluated.

Inflection	153,664	152,813	145,675	141,074	141,748	145,990	179,652	219,709
slope	1,000	10,000	25,000	50,000	75,000	100,000	200,000	300,000
2002	0.000	0.000	0.000	0.000	0.000	0.000	0.002	0.003
2003	0.000	0.001	0.003	0.006	0.008	0.011	0.020	0.026
2004	0.000	0.000	0.000	0.001	0.002	0.002	0.004	0.005
2005	0.438	0.438	0.438	0.438	0.438	0.438	0.438	0.438
2006	0.076	0.073	0.072	0.076	0.082	0.086	0.095	0.100
2007	0.000	0.000	0.001	0.001	0.002	0.002	0.004	0.005
2008	0.000	0.000	0.000	0.000	0.000	0.000	0.001	0.001
2009	0.000	0.000	0.000	0.000	0.000	0.001	0.002	0.004
2010	0.000	0.000	0.000	0.000	0.000	0.000	0.000	0.000
2011	0.022	0.023	0.023	0.022	0.022	0.022	0.024	0.024
2012	0.008	0.009	0.010	0.011	0.012	0.013	0.016	0.018
2013	0.013	0.013	0.014	0.018	0.020	0.021	0.023	0.024
2014	0.019	0.018	0.018	0.020	0.023	0.026	0.035	0.040
2015	0.000	0.000	0.000	0.001	0.002	0.004	0.011	0.014
2016	0.007	0.007	0.011	0.015	0.019	0.023	0.036	0.043
2017	0.000	0.000	0.001	0.004	0.005	0.006	0.009	0.011
2018	0.000	0.000	0.000	0.000	0.000	0.000	0.001	0.001

Table 2. Estimated red tide mortality on age-0 red grouper from July 2002 to March 2018. Mortality is expressed as the proportion of age-0 biomass killed by red tides for each of the mortality response curves evaluated.

Inflection	152,180	150,996	142,813	138,112	138,790	143,026	176,452	216,111
slope	1,000	10,000	25,000	50,000	75,000	100,000	200,000	300,000
2002	0.000	0.000	0.004	0.000	0.018	0.029	0.000	0.001
2003	0.034	0.037	0.070	0.045	0.106	0.129	0.052	0.060
2004	0.026	0.018	0.045	0.023	0.056	0.061	0.033	0.040
2005	0.412	0.411	0.418	0.410	0.441	0.454	0.409	0.412
2006	0.233	0.230	0.264	0.230	0.280	0.285	0.241	0.254
2007	0.000	0.000	0.016	0.003	0.030	0.037	0.007	0.011
2008	0.000	0.000	0.000	0.000	0.001	0.002	0.000	0.000
2009	0.000	0.000	0.003	0.000	0.009	0.014	0.000	0.001
2010	0.000	0.000	0.000	0.000	0.000	0.001	0.000	0.000
2011	0.114	0.115	0.143	0.128	0.138	0.133	0.140	0.144
2012	0.128	0.134	0.166	0.139	0.178	0.182	0.149	0.159
2013	0.161	0.163	0.200	0.176	0.197	0.192	0.192	0.198
2014	0.003	0.003	0.026	0.007	0.043	0.051	0.014	0.020
2015	0.000	0.000	0.040	0.007	0.061	0.070	0.020	0.031
2016	0.068	0.085	0.189	0.106	0.228	0.243	0.140	0.169
2017	0.036	0.036	0.057	0.039	0.070	0.077	0.047	0.052
2018	0.000	0.000	0.010	0.000	0.017	0.020	0.003	0.007

Table 3. Estimated red tide mortality on age 1-3 red grouper from July 2002 to March 2018. Mortality is expressed as the proportion of age 1-3 biomass killed by red tides for each of the mortality response curves evaluated.

Inflection	152,180	150,996	142,813	138,112	138,790	143,026	176,452	216,111
slope	1,000	10,000	25,000	50,000	75,000	100,000	200,000	300,000
2002	0.000	0.000	0.002	0.000	0.007	0.012	0.000	0.001
2003	0.000	0.003	0.034	0.014	0.059	0.075	0.021	0.027
2004	0.000	0.000	0.012	0.002	0.019	0.022	0.006	0.009
2005	0.494	0.494	0.498	0.494	0.505	0.508	0.496	0.496
2006	0.163	0.158	0.187	0.158	0.201	0.206	0.169	0.180
2007	0.000	0.000	0.015	0.004	0.022	0.025	0.009	0.012
2008	0.000	0.000	0.000	0.000	0.001	0.001	0.000	0.000
2009	0.000	0.000	0.002	0.000	0.007	0.009	0.000	0.001
2010	0.000	0.000	0.000	0.000	0.000	0.000	0.000	0.000
2011	0.088	0.087	0.076	0.087	0.072	0.071	0.082	0.078
2012	0.049	0.056	0.072	0.061	0.078	0.080	0.065	0.069
2013	0.080	0.080	0.095	0.082	0.096	0.094	0.090	0.094
2014	0.015	0.015	0.029	0.017	0.041	0.048	0.020	0.024
2015	0.000	0.000	0.015	0.000	0.031	0.039	0.003	0.009
2016	0.042	0.043	0.093	0.049	0.122	0.134	0.063	0.079
2017	0.000	0.000	0.019	0.003	0.031	0.036	0.010	0.015
2018	0.000	0.000	0.002	0.000	0.005	0.006	0.000	0.001

Table 4. Estimated red tide mortality on age 4+ red grouper from July 2002 to March 2018. Mortality is expressed as the proportion of age 4+ biomass killed by red tides for each of the mortality response curves evaluated.

Inflection	152,180	150,996	142,813	138,112	138,790	143,026	176,452	216,111
slope	1,000	10,000	25,000	50,000	75,000	100,000	200,000	300,000
2002	0.000	0.000	0.000	0.000	0.001	0.002	0.000	0.000
2003	0.000	0.000	0.007	0.002	0.014	0.019	0.004	0.005
2004	0.000	0.000	0.001	0.000	0.002	0.003	0.000	0.000
2005	0.433	0.433	0.433	0.433	0.432	0.432	0.433	0.433
2006	0.061	0.059	0.071	0.058	0.079	0.084	0.063	0.068
2007	0.000	0.000	0.000	0.000	0.001	0.002	0.000	0.000
2008	0.000	0.000	0.000	0.000	0.001	0.001	0.000	0.000
2009	0.000	0.000	0.000	0.000	0.002	0.003	0.000	0.000
2010	0.000	0.000	0.000	0.000	0.000	0.000	0.000	0.000
2011	0.012	0.012	0.013	0.012	0.016	0.017	0.012	0.012
2012	0.001	0.001	0.004	0.001	0.006	0.008	0.002	0.003
2013	0.002	0.002	0.009	0.003	0.011	0.012	0.006	0.007
2014	0.020	0.019	0.026	0.019	0.035	0.039	0.020	0.023
2015	0.000	0.000	0.003	0.000	0.008	0.011	0.001	0.002
2016	0.001	0.002	0.013	0.005	0.023	0.029	0.007	0.009
2017	0.000	0.000	0.005	0.001	0.006	0.007	0.003	0.004
2018	0.000	0.000	0.000	0.000	0.000	0.000	0.000	0.000

Figures

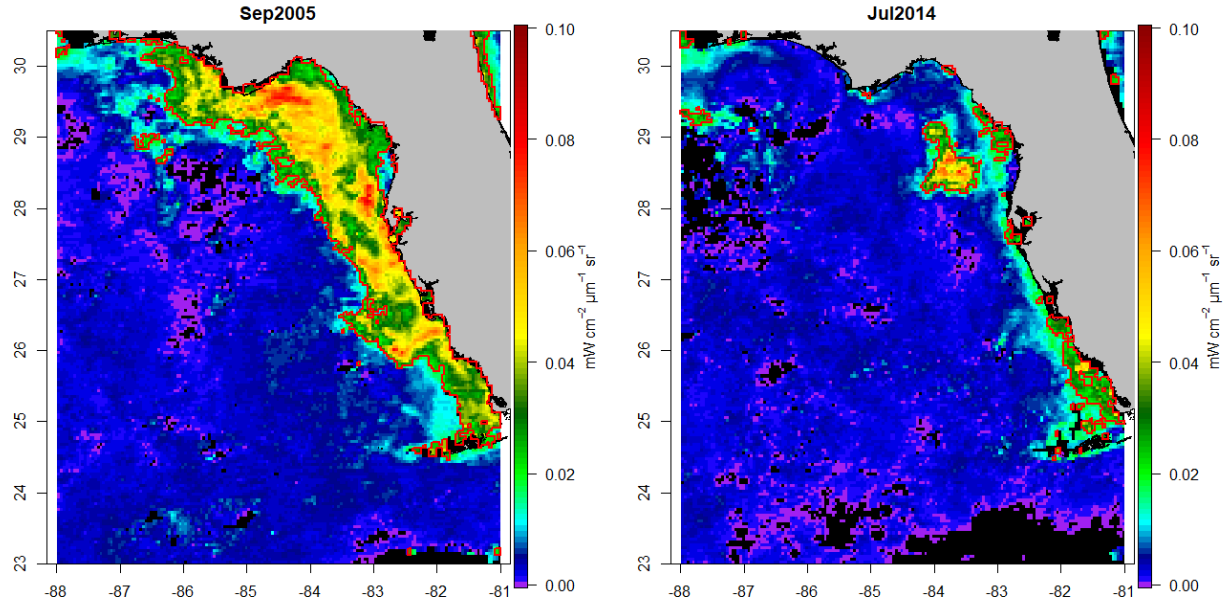

Figure 1. Florescent line height imagery (FLH) of the WFS in September 2005 and July 2014 with polygons identifying probable harmful algal blooms (FLH > 0.02).

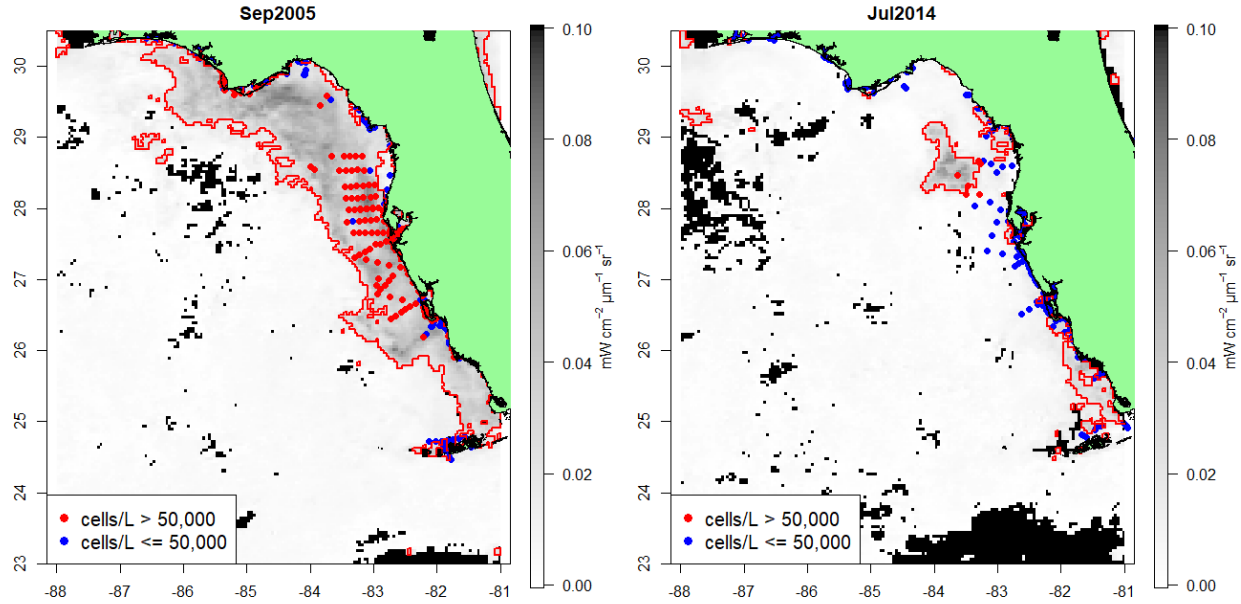

Figure 2. HAB sample locations above and below 50,000 cells/L overlaid with FLH imagery for September 2005 and July 2014.

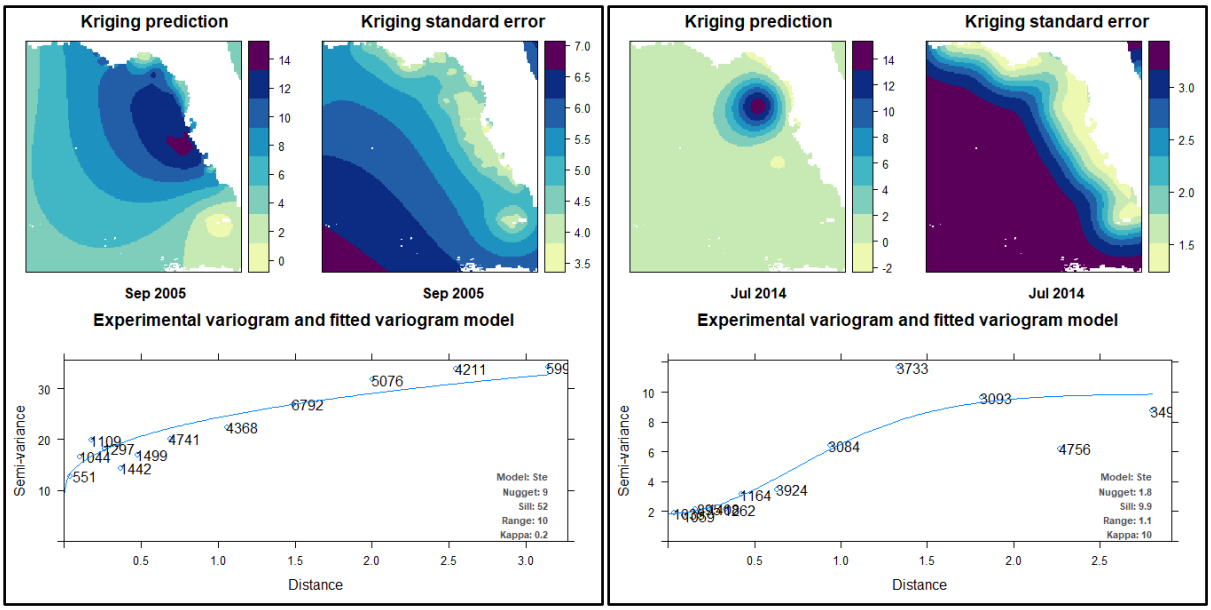

Figure 3. Predicted cell concentrations (log cells/L), standard error, and fitted variogram model from kriging the FWRI HAB monitoring data, September 2005 and July 2014.

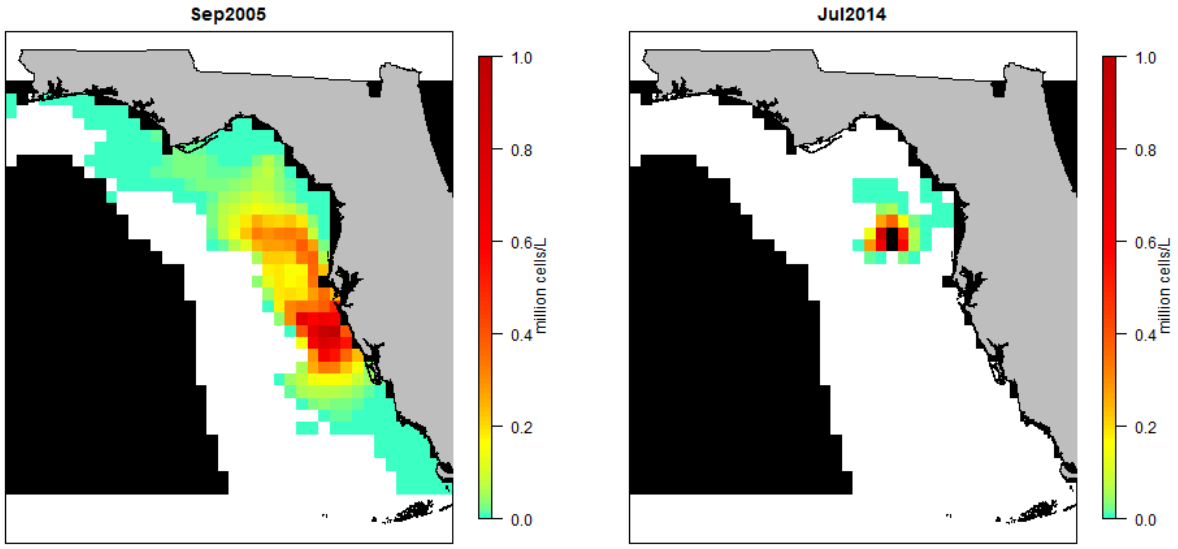

Figure 4. Final red tide maps used in the mortality analysis for September 2005 and July 2014. These maps are the kriged HAB data, clipped to the FLH imagery above the detection threshold of 0.02 and resampled to match the resolution of the species distribution maps from Ecospace.

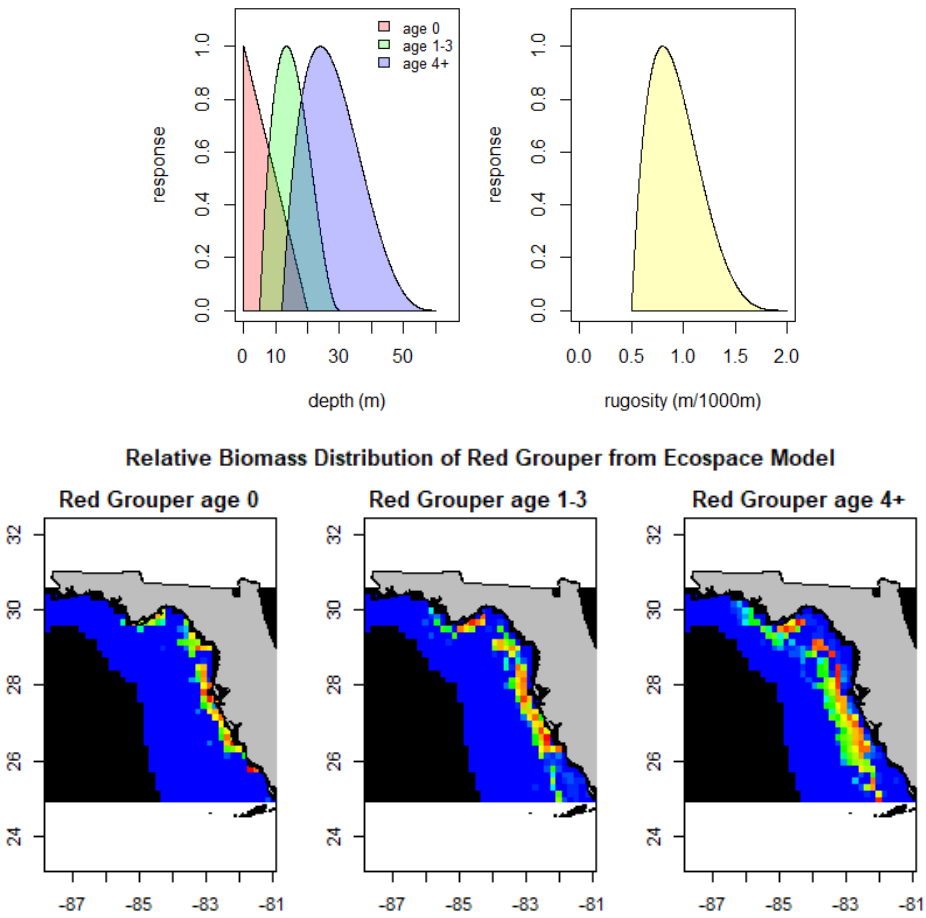

Figure 5. Depth and rugosity functions used for red grouper in the WFS Ecospace habitat capacity model (top panel) and resulting biomass distribution maps (bottom panel).

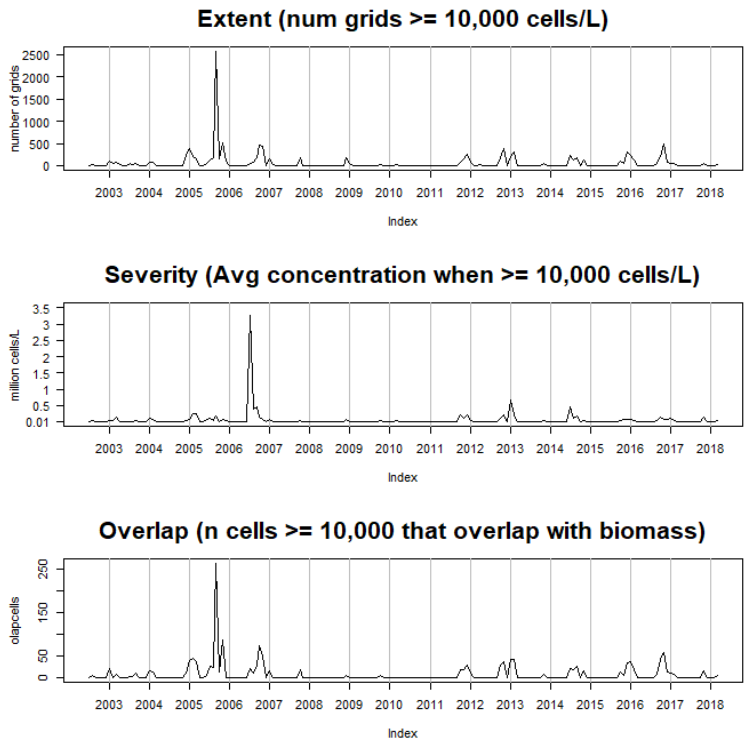

Figure 7. Summary of red tide blooms from July 2002 to March 2018 based on FLH satellite imagery and kriged FWRI-HAB monitoring data.

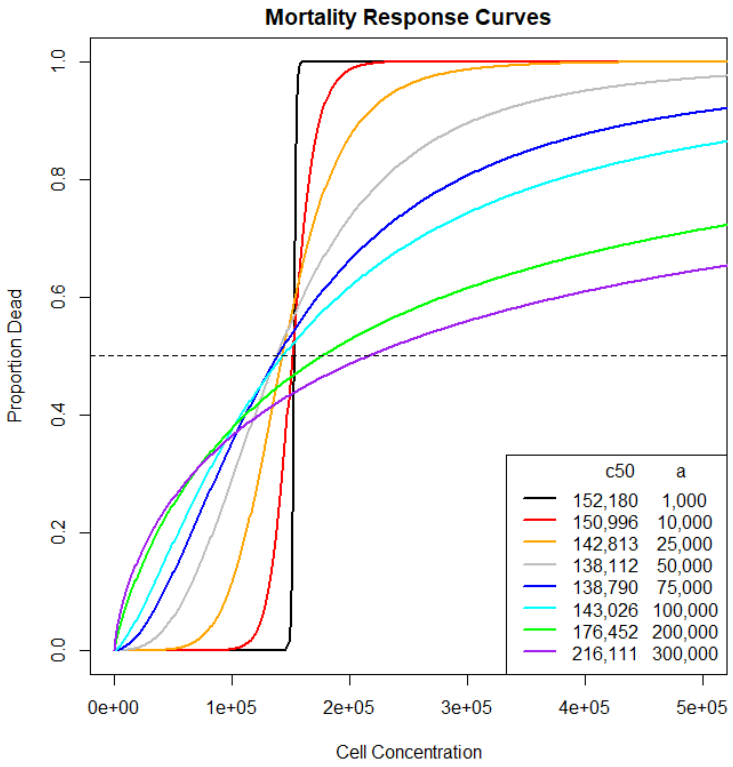

Figure 8. Mortality response curves that generated a red tide mortality rate of 0.438 in 2005 for red grouper. Note that the slope parameter in the logistic equation is scaled as $c50/a$, such that lower values of a result in steeper slopes.

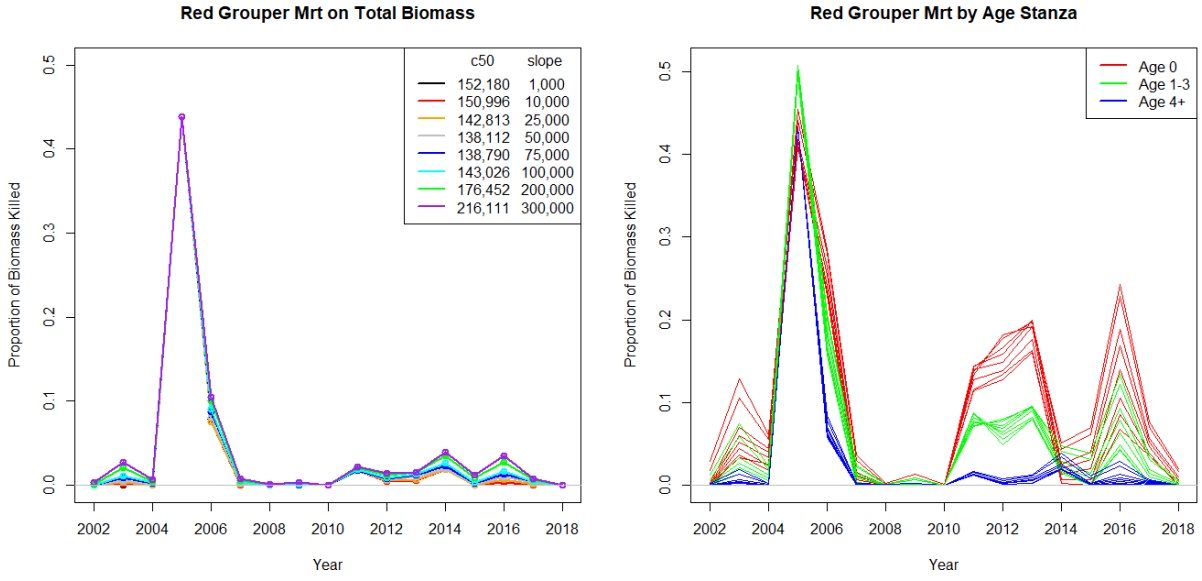

Figure 9. Estimated trend in red tide mortality on red grouper from July 2002 to March 2018. Here, mortality is expressed as the proportion of the total biomass killed (left panel) and the proportion of biomass killed in each age stanza by red tides in each year. In the age stanza plots, multiple lines correspond to the different response curves evaluated.

References

Acker, J. G., and G. Leptoukh. 2007. Online analysis enhances use of NASA earth science data. *Trans., Am. Geophys. Union* 88(2): 14-17.

Chagaris, D. 2013. Ecosystem-based evaluation of fishery policy options and tradeoffs on the West Florida Shelf. University of Florida, Gainesville, FL.

Chagaris, D. D., B. Mahmoudi, C. J. Walters, and M. S. Allen. 2015. Simulating the Trophic Impacts of Fishery Policy Options on the West Florida Shelf Using Ecopath with Ecosim. Marine and Coastal Fisheries 7(1):44-58.

Christensen, V., and coauthors. 2014. Representing Variable Habitat Quality in a Spatial Food Web Model. Ecosystems 17(8):1397-1412.

Flaherty, K. E., and J. H. Landsberg. 2011. Effects of a persistent red tide (*Karenia brevis*) bloom on community structure and species-specific relative abundance of nekton in a Gulf of Mexico estuary. Estuaries and Coasts 34: 417-439

Geselbracht, L. 2007. Conservation action plan for marine and estuarine resources of the Big Bend Area of Florida. The Nature Conservancy, Florida Chapter.

GMFMC. 2015. Standing, reef fish, and mackerel SSC meeting summary. Tab B, No. 4. Tampa, FL. Available online https://public.gulfcouncil.org:5001/sharing/bKayrmFlo.

Hu, C., F. E. Muller-Karger, C. J. Taylor, K. L. Carder, C. Kelble, E. Johns, and C. A. Heil. 2005. Red tide detection and tracing using MODIS fluorescence data: A regional example in SW Florida coastal waters. Remote Sensing of Environment 97(3):311-321.

Hu, C., B. B. Barnes, L. Qi, and A. A. Corcoran. 2015. A harmful algal bloom of Karenia brevis in the Northeastern Gulf of Mexico as revealed by MODIS and VIIRS: a comparison. Sensors 15(2):2873-2887.

Kirkpatrick, B., L. E. Fleming, D. Squicciarini, L. C. Backer, R. Clark, W. Abraham, J. Benson, Y. S. Cheng, D. Johnson, R. Pierce, and J. Zaias. 2004. Literature review of Florida red tide: implications for human health effects. Harmful Algae 3(2):99-115.

Landsberg, J. H. 2002. The effects of harmful algal blooms on aquatic organisms. Reviews in Fisheries Science 10(2):113-390.

Larkin, S. L., and C. M. Adams. 2007. Harmful algal blooms and coastal business: economic consequences in Florida. Society and Natural Resources 20(9):849-859.

SEDAR. 2009. SEDAR 10 Update - Gulf of Mexico gag Grouper stock assessment report. SEDAR, North Charleston, SC. Available online at: http://sedarweb.org/.

SEDAR. 2014. SEDAR 33 - Gulf of Mexico gag Grouper stock assessment report. SEDAR, North Charleston, SC. Available online at: http://sedarweb.org/.

SEDAR. 2015. SEDAR 42 - Gulf of Mexico red grouper stock assessment report. SEDAR, North Charleston, SC. Available online at: http://sedarweb.org/.

Smith, G.B. 1975. The 1971 red tide and its impact on certain reef communities in the mid-eastern Gulf of Mexico. Environ. Lett. 9:141–152.

Smith, G.B. 1979. Relationship of eastern Gulf of Mexico reef-fish communities to the species equilibrium theory of insular biogeography. J. Biogeogr. 6:49–61.

Soto Ramos, I. M. 2013. Harmful algal blooms of the West Florida Shelf and Campeche Bank: visualization and quantification using remote sensing methods.

Steidinger, K. A. 2009. Historical perspective on Karenia brevis red tide research in the Gulf of Mexico. Harmful Algae 8(4):549-561.

Steidinger, K. A., and R. M. Ingle. 1972. Observations on the 1971 summer red tide in Tampa Bay, Florida. Environmental Letters 3(4):271-278.

Walsh J. J., J. K. Jolliff, B. P. Darrow, J. M. Lenes, S. P. Milroy, A. Remsen, D. A. Dieterle, K. L. Carder, F. R. Chen, G. A. Vargo, R. H. Weisberg, K. A. Fanning, F. E. Muller-Karger, E. Shinn, K. A. Steidinger, C. A. Heil, C. R. Tomas, J. S. Prospero, T. N. Lee, G. J. Kirkpatrick, T. E. Whitledge, D. A. Stockwell, T. A. Villareal, A. E. Jochens, P. S. Bontempi. 2006. Red tides in the Gulf of Mexico: Where, when, and why? Journal of geophysical research 111: 1-46.

Walsh, J., R. H. Weisberg, J. M. Lenes, F. R. Chen, D. A. Dieterle, L. Zheng, K. L. Carder, G. A. Vargo, J. A. Havens, E. Peebles, and D. J. Hollander. 2009. Isotopic evidence for dead fish maintenance of Florida red tides, with implications for coastal fisheries over both source regions of the West Florida shelf and within downstream waters of the South Atlantic Bight. Progress in Oceanography 80(1-2):51-73.

Walter J, M. C. Christman, J. H. Landsberg, B. Linton, K. Steidinger, R. Stumpf, and J. Tustison. 2013. Satellite derived indices of red tide severity for input for Gulf of Mexico gag grouper stock assessment.SEDAR33-DW08. SEDAR, North Charleston, South Carolina, 43 pp.